AUTONOMOUS IDENTIFICATION OF MATRICES IN THE APNEA[a] SYSTEM

David Hensley
Oak Ridge National Laboratory, Oak Ridge, TN 37831

ABSTRACT

The *APNea* System is a passive and active neutron assay device which features imaging to correct for nonuniform distributions of source material. Since the imaging procedure requires a detailed knowledge of both the detection efficiency and the thermal neutron flux for (sub)volumes of the drum of interest, it is necessary to identify which mocked-up matrix, to be used for detailed characterization studies, best matches the matrix of interest. A methodology referred to as the external matrix probe (EMP) has been established which links external measures of a drum matrix to those of mocked-up matrices. These measures by themselves are sufficient to identify the appropriate mock matrix, from which the necessary characterization data are obtained. This independent matrix identification leads to an autonomous determination of the required system response parameters for the assay analysis.

INTRODUCTION

The material of a drum matrix interferes with neutron assays by modifying the efficiency with which signal neutrons from the drum are detected. It further affects active assay by modifying the interrogating thermal neutron flux, in intensity, spatial distribution, and temporal distribution. Since the imaging procedure used by the *APNea* System requires a detailed knowledge of both the detection efficiency and the effective thermal neutron flux, it is necessary to select characterization data which best match the character of the drum of interest — the characterization data provide the response information required by the *APNea* imaging algorithms. Eqs. 1,2 are two of the basic equations used, respectively, to perform passive and active imaging in the *APNea* System. (A detailed discussion of these and related equations is covered in Ref. 1.) The unknown source term for the drum subvolume V_b is $\rho(V_b)$, and $Y(d,\theta,t)$ is the measured yield. The system response functions are:

[a] *APNea* — It takes your breath away!

$\epsilon(d, V_c)$, the efficiency for detector d to see an epithermal neutron emitted from V_c, a chamber (sub)volume; $Flux(V_c, t)$, the thermal neutron flux available within V_c at the time t, relative to the neutron generator pulse; and $Fast(d, t)$, the detector response to the neutron generator pulse. The coefficients $A(d, \theta)$ normalize the $Fast$ function to the current drum matrix.

$$Y(d, \theta) = \epsilon(d, V_c) * \rho(V_b) \qquad \text{where } V_c = V_b(\theta) \tag{1}$$

$$Y(d, \theta, t) = \epsilon(d, V_c) * \rho(V_b) * Flux(V_c, t) + A(d, \theta) * Fast(d, t) \tag{2}$$

The imaging algorithms of Ref. 1 have the general property that the response functions need only be approximate for a good relative image to be obtained for both the passive and active assays, but it is painfully obvious that the absolute intensity of the image, i.e. the desired assay result, depends directly on the accuracy of the magnitude of the response functions. Since most of the information detailing the nature of the contents of a drum, either from generator manifests or from x-ray or γ-ray examination, does not address the neutronic properties of the drum matrix directly, it is necessary to have a method for determining independently the neutronic response information required for the assay analysis. What is described here is a methodology for using external probes and monitors to identify, in as direct a way as possible, the neutronic characteristics of a given matrix. This methodology, dubbed the external matrix probe (EMP), is not dependent on input from other sources, though it may be improved and/or verified by outside sources of information.

MOCK MATRIX

It is possible to mock up the gross properties of a matrix of interest fairly accurately. For example, a dirt matrix can be approximated by clean dirt from the same site, by similar dirt from that region, by similar dirt, period. The same applies for concrete rubble, Rashig

rings, compacted gloveboxs, or nasty Rocky Flats sludge. The mocked-up drum should then have gross properties reasonably close to those of the drum of interest. As an other aspect of mocking up the gross properties of the matrix, the same kind of drum should be used including any liner or special packing material such as large plastic bags. It is assumed (and required) that the mock matrix be azimuthally uniform, though it may be somewhat radially nonuniform. A bird cage or other central structure is an acceptable form of radial nonuniformity. The matrix may be grossly nonuniform in the vertical direction, though the more uniform it is the more straightforward the preparation for the analysis is. The typical vertical nonuniformity is a partially packed drum, i.e., the top is empty. A less desirable form results from layering a different kind of waste on top of existing waste, as is sometimes the case when waste is generated at a slow rate. Moisture settling to the bottom could lead to an especially annoying nonuniformity.

As mentioned previously, even at this initial level of mimicking, the corresponding response functions are such that an accurate source image of the unknown drum can be generated, although the overall intensity of the image will generally be uncertain. For the next level of mimicking the unknown matrix, the mock matrix can be fine tuned by varying the hydrogen content of the matrix, as this material most strongly affects epithermal signal neutrons and serves to thermalize the neutron generator pulse. Adding water or polyethylene (poly) to the matrix generates a series of mock matrices, all of which will have the gross properties of the drum of interest but which will differ slightly from one another because of the varied amounts of hydrogen. Then if one is sufficiently fortunate, the *optimum* mock matrix will be contained somewhere within this set of matrices. Notice that the mock matrices fall into two category levels. First they have gross properties such as being soil or concrete or glass. Second, they have subtle differences achieved by varying the hydrogen content. It should be appreciated that introducing incremental quantities of hydrogen into a matrix so that it is uniformly spread is not a simple task and that ultimately computer modeling of the matrix within the *APNea* Unit will be needed to meet the requirements of making arbitrary incremental changes to a mock matrix.

RESPONSE FUNCTIONS

What is done with each mock drum is to subject it to a number of internal measurements so as to fully characterize it and to obtain the response functions used by the *APNea* imaging algorithm. Fig. 1b shows a top view of a calibration drum with 5 tubes at various radial positions within which a ^{252}Cf source or a small thermal neutron detector can be positioned at various heights. The drum is then rotated through the eight θ segments. The full panoply of tubes to be calibrated is depicted in Fig. 1a. The ^{252}Cf point source positioned in the drum supplies $\epsilon(d, V_c)$, the absolute detection efficiency for each detector for each volume of interest. Fig. 2 shows the response of the N2 detector to an internal ^{252}Cf source as the source is positioned at various radial positions with respect to N2. Also (α,n) point sources can be used similarly to characterize the system for neutrons emitted with an energy spectrum different from that of fission neutrons. A thermal neutron detector positioned consecutively in each volume in the drum measures $Flux(V_c, t)$, the thermal neutron flux associated with the neutron generator pulses, where t is measured relative in time to the neutron generator pulse. The $Fast(d, t)$ function shape, which is observed to be matrix independent, can be verified, and the $Fast$ normalization coefficients, $A(d, \theta)$, for this matrix can be obtained.

In addition to the characterization measurements, the mock drum is subjected to the full panoply of *APNea* System measurements, active, passive and EMP. The EMP and assay measurements will be shown to link some appropriate mock matrix (matrices) to the matrix of interest. The goal of this paper is to establish the link between *APNea* System measurements (external measures) and the response functions (internal characteristics) used to image and calculate the assay results.

EMP MEASURES FOR THE DETECTION RESPONSE

Two basic measurements, EMP(Xmit) and EMP(Scatter), are made to identify the appropriate mock matrix which is to supply $\epsilon(d, V_c)$, the detection efficiency response information

Mock Matrices

Matrix	$\Sigma Y(0,18)$		Flux	Description
	Liner	Bare		
MT	-	1711	'21365	Empty chamber
MTD	1725	-	27901	Empty lined drum
S	1730	1812	'2364	670 lbs of steel shot
RR	1704	-	<4	Mint condition Raschig rings
SS	-	1698	-	1740 lbs steel shot
S47	931	1057	'2499	47 lbs poly, 685 lbs steel
SOIL	618	-	14368	420 lbs NFS soil
CONC	-	400	'23230	920 lbs ORNL concrete
S140	330	411	'8974	140 lbs poly, 555 lbs steel

Table 1:

for the drum of interest. With a ^{252}Cf source positioned at various heights outside but near the drum, transmission measurements are made with three different detectors, a vertical wall detector N2, a bottom detector B2, and a top detector T2, leading to EMP(N2), EMP(B2), and EMP(T2), respectively. (See Fig. 1a for a schematic picture of the various detector packs.) The advantages of the three different choices will be discussed in Ref. 2. The scattering of neutrons off the drum matrix is measured as EMP(S1S2) by a pair of detectors, S1 and S2, behind the point source. Features of these EMP measurements are very similar to measurements that occur as part of the characterization studies. The EMP(N2) measurement, for example, is simply an extension to a point outside the drum of the internal measurements of Fig. 2 — it would be a point on this plot at $(r,h) = (-14,18)$. As depicted schematically in the linear plot in Fig. 2a, the EMP measurement covers only a small part of the N2 detector's dynamic range, but, as depicted in the semi-log plot in Fig. 2b, the dynamic range of this measurement must still be very large, covering over an order of magnitude.

There are two key questions to be addressed as to whether the EMP(Xmit) measurement is sensitive to what the elements of $\epsilon(d,V_c)$ are. One, does it reflect what the detection

efficiency for the core is? This is a crucial questions as an external measure may be only loosely correlated with this (totally) internal response. Fig. 3a plots EMP(N2) against N2(0,18), the response of detector N2 to a point source at (0,18) in matrices described in Tab. 1. Names in the figure with an apostrophe appended indicate mock drums which didn't have a plastic liner as was later used in all of the drums shipped to the *APNea* for assay. The empty-like matrices above 70% transmission in Fig. 3a don't have any useful relationship to EMP(N2). The points in the expanded Fig. 3b between 20% and 40% transmission appear to be correlated in a meaningful way, but it must be realized that the total core detection efficiencies listed in the table are nearly maximum for the various matrices down through *SS*, when compared with the *MT* matrix. Above $N2(0,18) = 15000$ there is so little loss of signal neutrons, overall, that comparing efficiency measurements with transmission measurements makes little sense. These matrices have so little hydrogen in them that, while neutrons may scatter, they don't get moderated and then absorbed. Below EMP(N2)=20%, however, there is an excellent correlation between EMP(N2) and the detection efficiency for the core of the matrices.

But the second questions has to do with N2(8,18) and N2(10,18), because the detection efficiency for detector positions near the front edge of a drum clearly are very important for imaging material in the annulus. Fig. 3c shows the relationship between EMP(N2) and N2(10,18). Here the results are much less clear than those for N2(0,18). There is a reasonable correlation for many of the interesting matrices, but the unusual brightness of concrete has raised the *CONC* response far above the *S140* response, even though they have essentially the same EMP(N2) value. It was discussed in Ref. 1 that this effect arises from different scattering properties of the two matrices, and this result points out the difficulty of defining a property by a measure that deals with a quite different property. A transmission measurement is more affected by out-scattering, moderating, and absorbing, whereas the scattering measurement is affected by in-scatter but little at all by absorbing or moderating. For that reason an additional measure, EMP(S1S2), was included. This particular measure now groups the matrices differently, as in Fig. 3d. Matrices with the greater scattering

brightness stand out well and are identified.

The conclusion is that it requires both EMP(Xmit) and EMP(Scatter) to identify the gross properties of the passive matrix correctly, though generally, it will be EMP(Xmit) which defines the fine features of the matrix. The combination of the two measures pins down the actual neutronic properties of scattering, moderating, and absorbing that the matrix exhibits. EMP(Xmit) defines the back annulus very well and the core fairly well, but experiences some ambiguities for the front annulus. EMP(Scatter) then clarifies the response for the front annulus.

EMP MEASURE FOR THE THERMAL FLUX RESPONSE

Fig. 4 depicts some of the internal thermal neutron flux information available from the active characterization studies. The upper plot shows the distribution of flux in a drum, where the neutron generator (NG) is indicated schematically to be on the right. The thermal flux (integrated beginning at $300\mu s$) is generally flat for the two empty matrices but drops from front to back for actual matrices. The amount of flux is related to the amount of hydrogen in the matrix. The steel based matrices have less internal flux as their hydrogen loading drops from *S140* to *SS*. There is almost as little flux at the center of the *SS* matrix as there is in the *RR* matrix. Flux leaks in from the *APNea* cavity, and this influx is most evident at back positions for the weaker flux matrices, as the flux profile begins to increase at back positions. The dieaway time information in the lower plot exhibits a clear minimum at $r = 0$. All matrices show an increase in dieaway time at back positions where there is less fast matrix flux mixing with the slower cavity flux penetrating the drum. The cavity dieaway time is typically at least $200\mu s$ slower than that within the matrix. The times for the very low flux matrices are difficult to calculate as many of the yields were so low.

Fig. 5 shows some of these details in a different way. Fig. 5a shows the correlation between flux measured in the front section of the drum, F(+), versus the flux in the center of the drum, F(0), and the flux in the back section, F(−). The three flux profiles are clearly well

correlated. The three other plots show the dieaway time responses in the various sections of the drum versus the flux results of Fig. 5a. Dieaway times, T(0) and T(+), correlate well with flux for the four higher-flux matrices but the relationship becomes chaotic for the three low flux cases. T(−), the dieaway time for the back section of a drum in Fig. 5c, is not particularly well correlated with the flux magnitudes for any of the matrices — so much cavity flux has leaked in that one is measuring largely cavity-flux times rather than matrix-flux times.

To determine the appropriate thermal flux response, several EMP parameters are studied. The most important come from the drum flux monitors (DFM), thermal-neutron flux monitors which are shielded to be sensitive only to the surface of the drum and not to the cavity walls. Of lesser importance are cavity flux monitors (CFM) which monitor flux in the space between the drum and the chamber walls but which are not shielded from the walls. In both cases, the flux measured by these monitors is analyzed for its time dependence in addition to its magnitude. Fig. 6 shows the correspondence between the internal flux and some of the external flux monitors, and Fig. 6a identifies the corresponding matrices. There is a very usable correlation between external flux and internal flux for DFMs in Fig. 6a,b,c and even for CFMs, though the CFM results in Fig. 6d exhibit some ambiguity. Especially pleasing is the correlation with the drum core flux, F(0), since one wants the external measure to correlate well with the totally internal parameter. The correlation with F(−) is acceptable but somewhat problematical.

An interesting parameter might be the time dependence of the flux monitors, themselves. Fig. 7 shows the correlation between the internal flux and the dieaway time of the flux monitors, with matrices identified in Fig. 7c. The prognosis for using the monitor dieaway times is reasonably good for predicting both F(0) and F(+) as seen in the figure for matrices from *S47* up. The scatter in the DFM(4) results in Fig. 7a arise from fitting data with low couting statistics. The results for F(−) are less clear and are indicative of the care which must be exercised in order to identify the appropriate gross matrix. For *S* and below, the

leak-in of cavity flux distorts the results too much for most of the monitor times to be useful. DFM(6), a monitor viewing the surface of the drum away from the generator, appears to give interesting and useful results for the low flux matrices.

Since the desired flux response function, $Flux(V_c, t)$, is a function of the time relative to the neutron generator pulse, it is important that the time character of the internal flux be identified. Ref. 1 discusses how the time variation of this function affects the ability of the imaging algorithm both to image the core of the drum and to separate out the *Fast* interference for times under $700\mu s$. Fig. 8 compares the external monitor flux measurements with the internal flux dieaway times, with matrices identified in Fig. 8a. The DFM results for *S47* and above are reasonable for T(0) and T(+). But, as usual, results for the weaker flux matrices are ambiguous and results for all T(−) data are complicated and confusing. In this comparison, the CFM time results in Fig. 8d are not nearly as useful as were the CFM flux correlations to the internal flux.

Fig. 9 compares the monitor dieaway times with those of the internal flux. Fig. 9a compares the dieaway times of six monitors with T(0), the internal dieaway time at the core. Notice that the CFM monitor times are several hundred microseconds longer than the times for the DFM due to the longer dieaway time of the cavity. Again, the results are good for *S47* and above, but turn around for the weaker flux matrices. The matrices are identified in Fig. 9d. The correlation for T(+) in Fig. 9d is also quite good, but there is little if any simple correlation for T(−) in Fig. 9b. It is likely that pinning down the dieaway time of the back drum section will require comparing the DFM results to those of the CFM to predict what the mix of the two flux types is. Fortunately, the DFM results seem to specify the back section flux fairly well, so specifying the back section dieaway times should be possible.

The dieaway times referred to up till now are single exponential fits to the data. It would be unreasonable to expect that a single dieaway component is contributing, so this approach is, at best, an approximation. Ref. 2 will discuss this point in more detail, as it affects the accuracy with which the flux function can be designated.

Another interesting measure is the amount of the neutron generator pulse which is either scattered off or transmitted through the drum matrix. The $A(d, \theta)$ coefficients in Eq. 2 gives these measures. A(N2) is a beam transmission measure and A(S1,S2) is a beam scatter measure. These measures are of interest since they are the result of interactions with a primary 14 MeV neutron pulse and not with the much lower energy fission neutrons. An additional parameter being studied is the time dependence of the signal detectors, since their response is related directly to the decay time of thermal flux in the drum. Both of these measures appear to have worthwhile applications, but a detailed discussion of their character would overwhelm this paper.

SELECTING A MATRIX

Fig. 10 compares the EMP measures for various calibration matrices with measurements from an actual campaign of drums. Fig. 10a shows the basis for the selection of the matrix for the efficiency response. The three campaign matrices shown here are soil, concrete rubble, and Rachig rings. The EMP(S1S2) brightness of soil and Rachig rings is about the same, near 140%, but the concrete rubble lies at a noticeably higher value, though not as high as the 165% value for *CONC*. It seems quite reasonable that the concrete rubble would not scatter as many neutrons from its surface as would the solid concrete. After the scattering property is determined, then one looks to the EMP(N2) axis for the transmission value. The soil matrices lie within the range of the *CONC*, *SOIL*, and *S147* matrices. The concrete rubble has a somewhat higher transmission, so the appropriate matrix for it, in this case, would be a combination of the previous three matrices and the *S47* matrix.

Figs. 10b,c,d show the EMP determination of the calibration matrix for the flux response. The mock matrices are indicated in the figures along with the campaign matrices. Rachig rings lie in a clear section of the plot where minimal flux is detected. The concrete rubble and the soil have different responses, depending on which flux monitor is chosen, but they would fit a flux response similar to that of *SOIL* and *CONC*. In these figures it was possible

to draw a line that follows the increase in the internal flux. This is particularly helpful when one is dealing with a situation as with DFM(6) in Fig. 10d. Here the mock values clearly bend around and knowing how to follow the values can be very valuable. DFM(5) is looking at the generator side of the drum, and DRM(6) is looking at the back of the drum. The dieaway times for DFM(5) are lower and closer to the actual internal dieaway times. DFM(6), by looking at the back of the drum, is much more sensitive to the influx of cavity flux, and it records a somewhat longer dieaway time. The combination of these two measures enable one to specify the front and back internal flux response as well as to fix the absolute value of the internal flux. There are difficulties with the actual monitor values which will be discussed in Ref. 2.

CONCLUSIONS

Since one recognizes the importance of the response functions to the final assay results, the necessity of a way to specify these functions becomes apparent. The *APNea* System has focused on three different but related goals. One goal has been to provide an accurate image, accurate particularly in relative terms as was discussed in Ref. 1. The companion goal has been to understand the properties of the *APNea* Unit and of the drum assay problem so that mock matrices could be constructed that would supply the appropriate and necessary response functions. This will not be an easy goal to achieve, since the generating of mock matrices is a complicated challenge. The final goal has been to provide a defensible method for identifying the fine-tuned response functions necessary for providing an accurate absolute image. The EMP methodolgy depends on understanding the internal matrix characteristics and to relating them to crucial external measures. Within a reasonable dynamic range of matrices, the EMP methodolgy lays the foundation for an independent identification of the neutronic characteristics of drums encountered in nondestructive assay situations where the matrices cannot be directly examined. Determining and understanding the underlying uncertainties in the final results constitute an exhausting endeavor which will be addressed

in Ref. 2. But the current methodology gives strong optimism that accurate and believable results can be delivered by a method which is essentially independent of outside crutches.

ACKNOWLEDGMENTS

Larry Pierce was instrumental in fabricating the several mock matrices which were used in this study. Even though he was not a happy camper when it came time to mix in various quantities of dusty and choking vermiculite, he came up with good methods that provided quality mock matrices. Jim Madison and Sherry Williams, who are tasked to the daily operation of the *APNea* Unit, provided invaluable assistance in obtaining the bulk of the characteriation and EMP information.

Oak Ridge National Laboratory is managed by Lockheed Martin Energy Systems, Inc. for the U.S. Department of Energy under contract no. DE-AC05-84OR21400. The submitted manuscript has been authored by a contractor of the U.S. government. Accordingly, the U.S. Government retains a nonexclusive, royalty-free license to publish or reproduce the published form of the contribution or allow others to do so for U.S. Government purposes.

REFERENCES

1. D.C. Hensley, "Source Imaging of Drums in the *APNea* System," submitted to the *4th Nondestructive Assay and Nondestructive Examination Waste Characterization Conference*, Salt Lake City, Utah (October 24, 1995).

2. D.C. Hensley, "Uncertainty Considerations in the *APNea* System," submitted to the *4th Nondestructive Assay and Nondestructive Examination Waste Characterization Conference*, Salt Lake City, Utah (October 24, 1995).

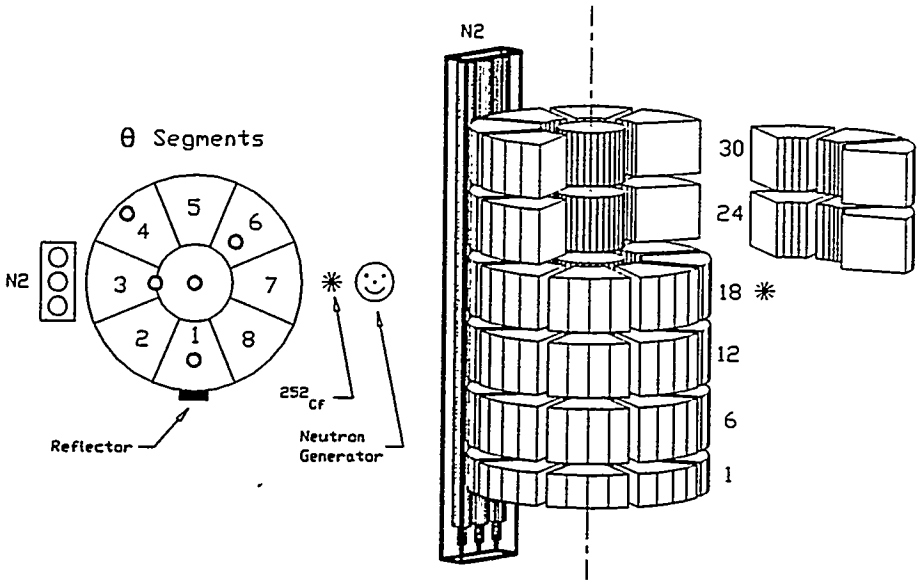

Figure: 1b) Schematic view of imaging voxels.

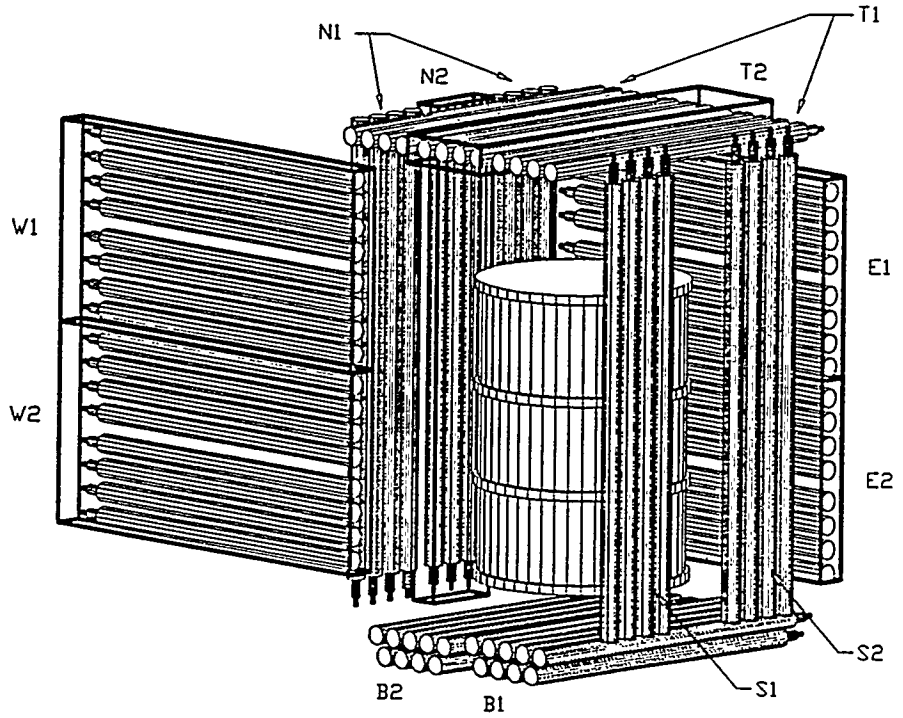

Figure: 1a) ^{3}He tube placement in the APNEA.

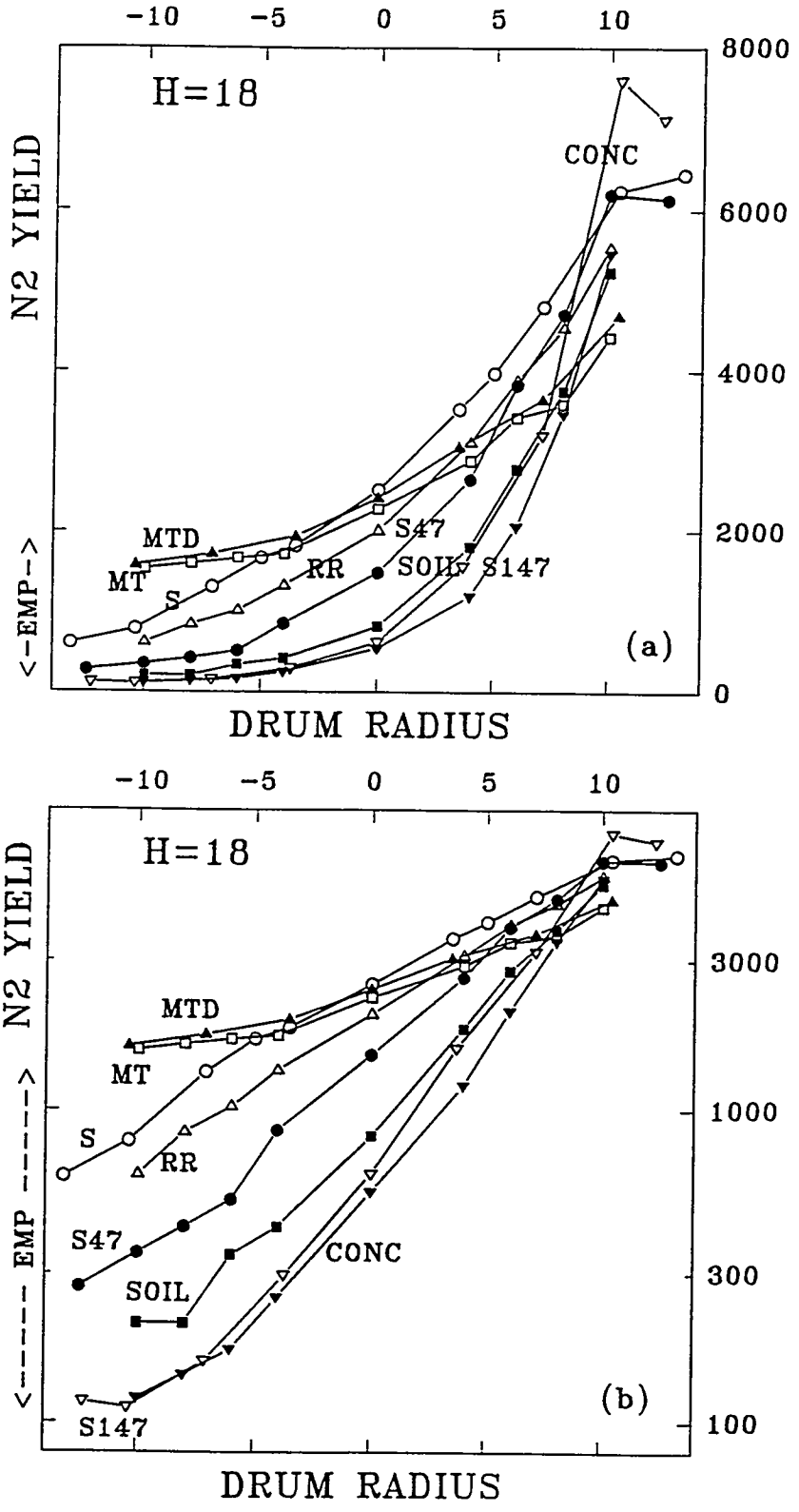

N2 DETECTOR RESPONSE TO AN INTERNAL SOURCE

FIGURE 2

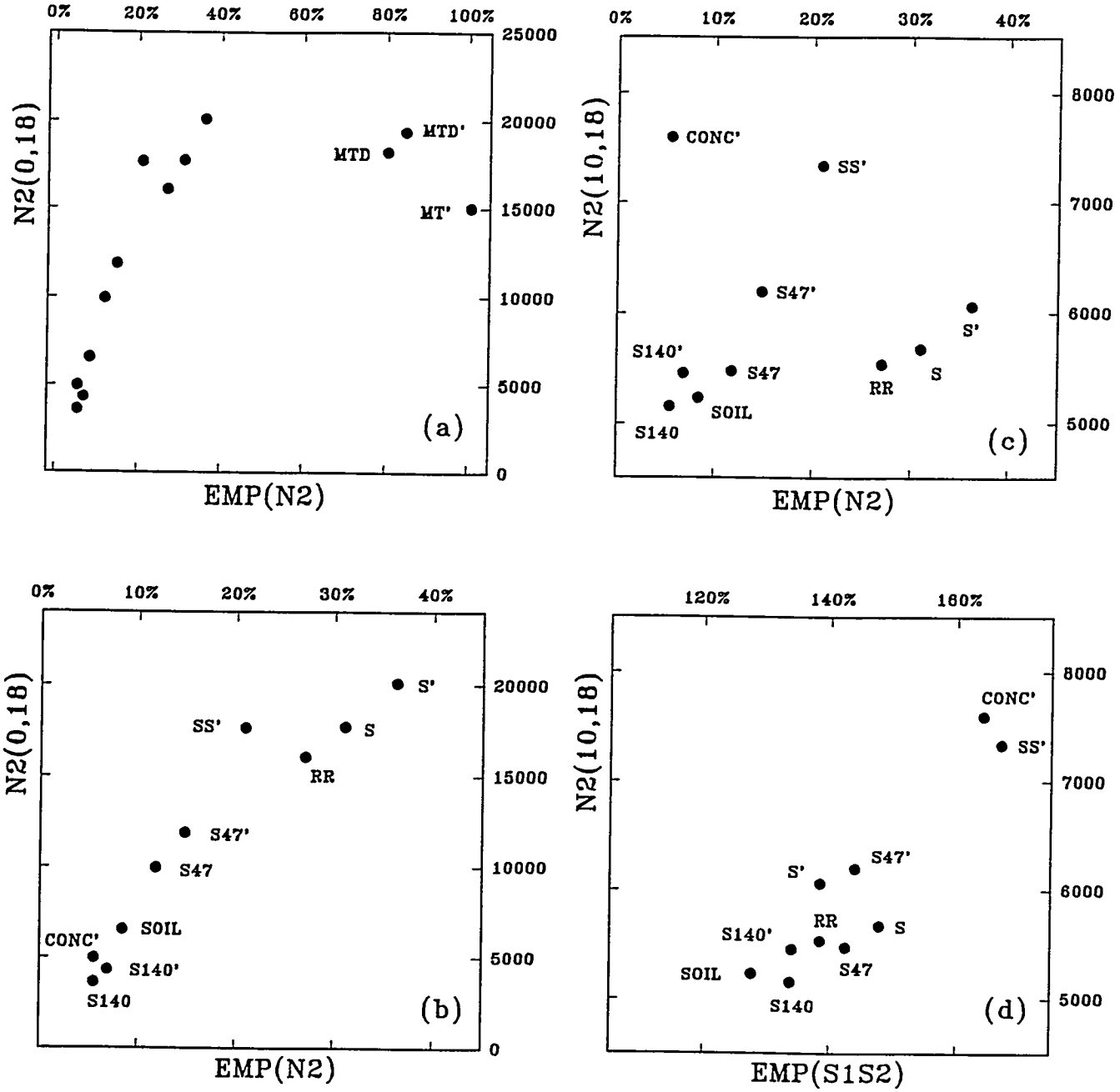

EMP(N2) AND EMP(S1S2) COMPARED TO N2 RESPONSES

FIGURE 3

DISCLAIMER

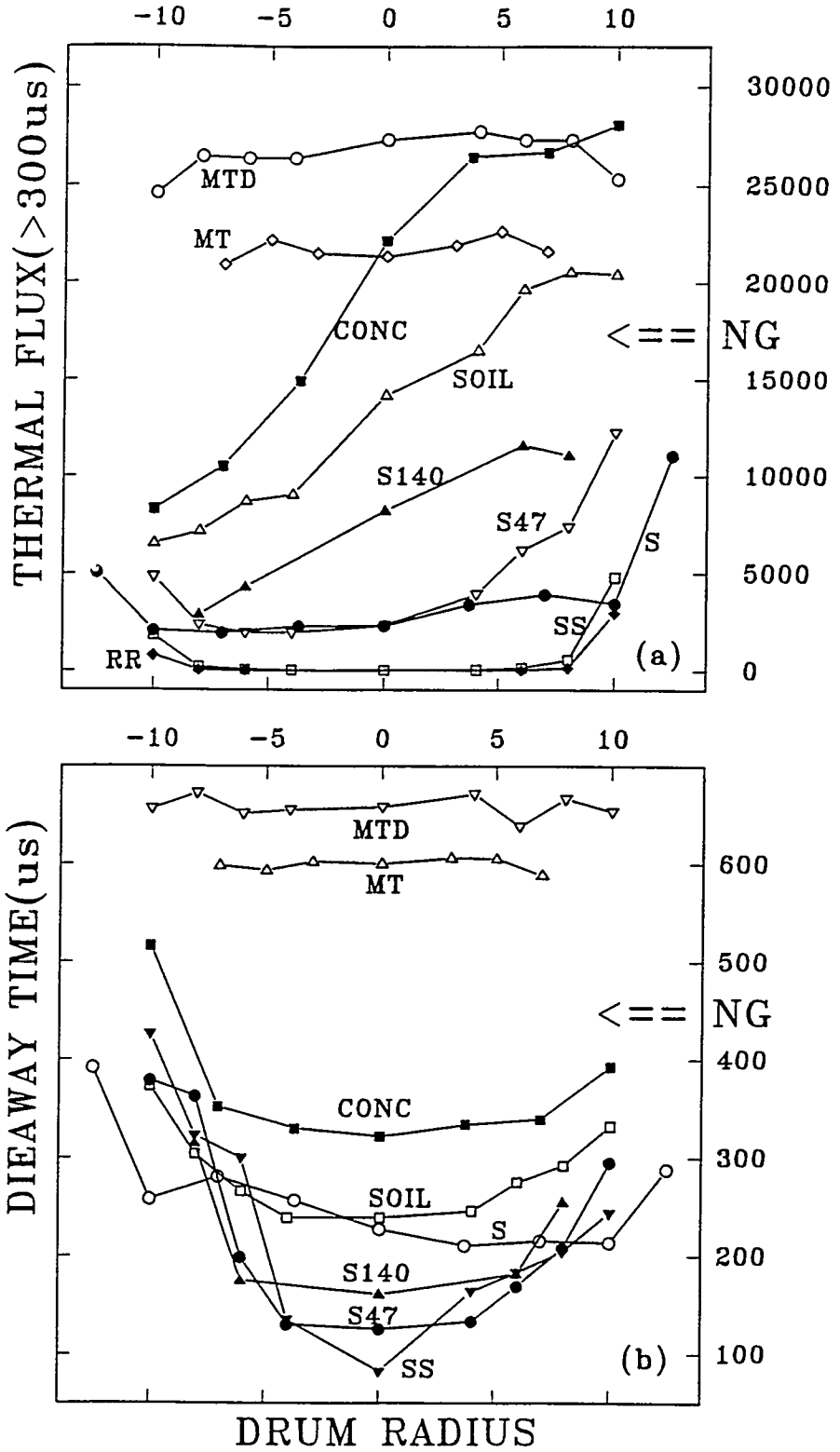

INTERNAL FLUX AND DIEAWAY TIMES

FIGURE 4

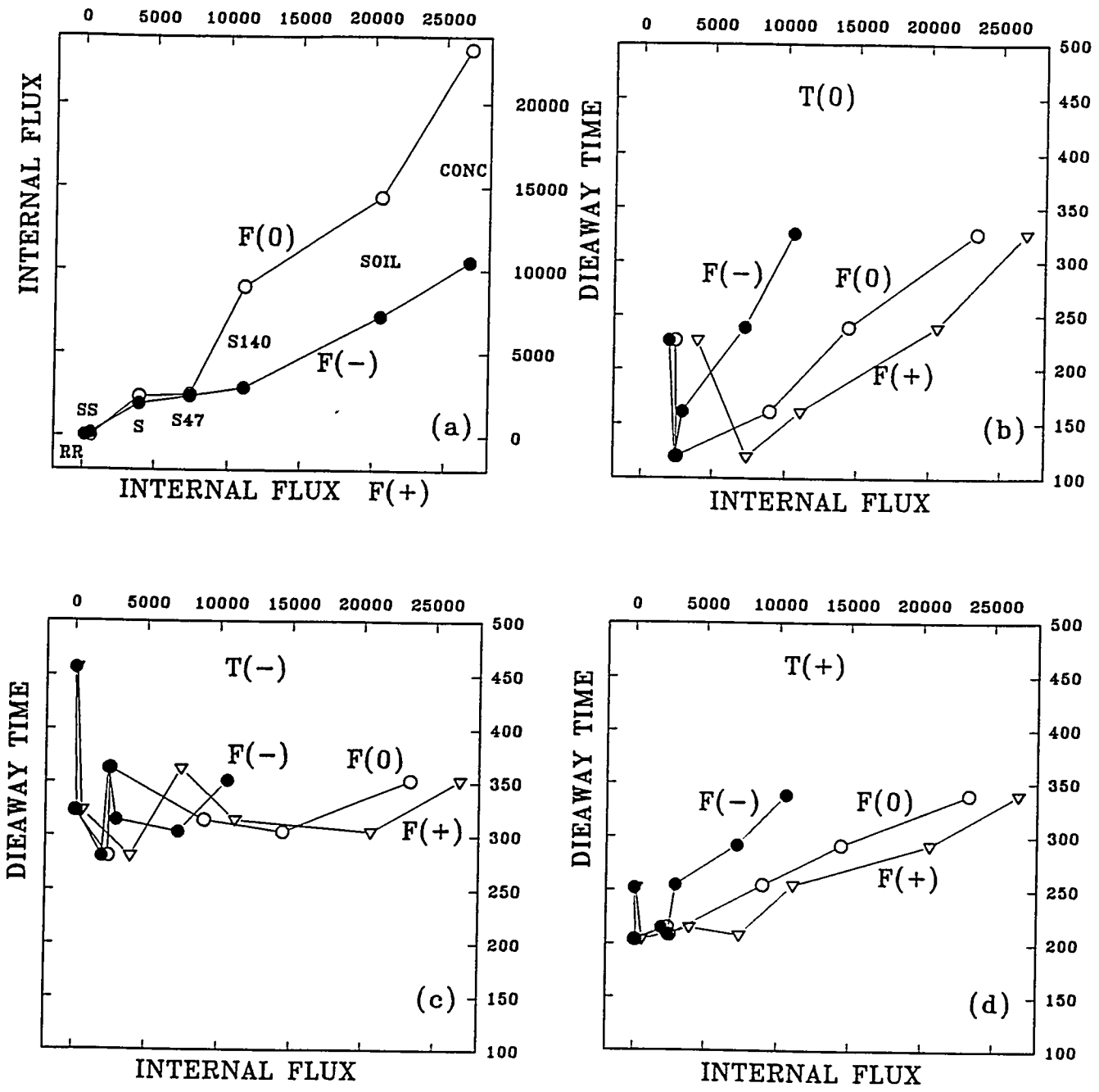

INTERNAL FLUX AND DIEAWAY TIME CORRELATIONS

FIGURE 5

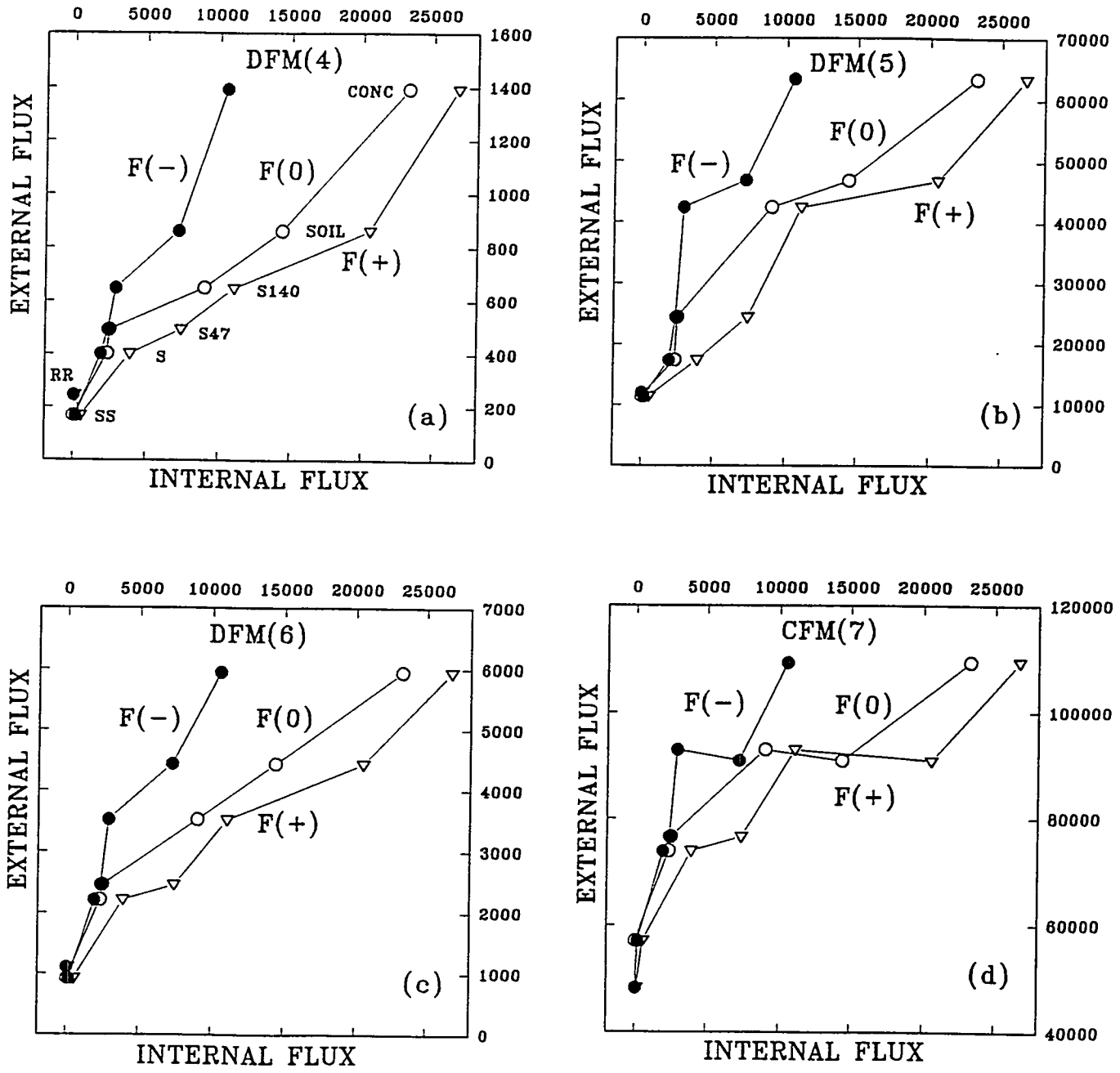

INTERNAL FLUX VERSUS EXTERNAL FLUX

FIGURE 6

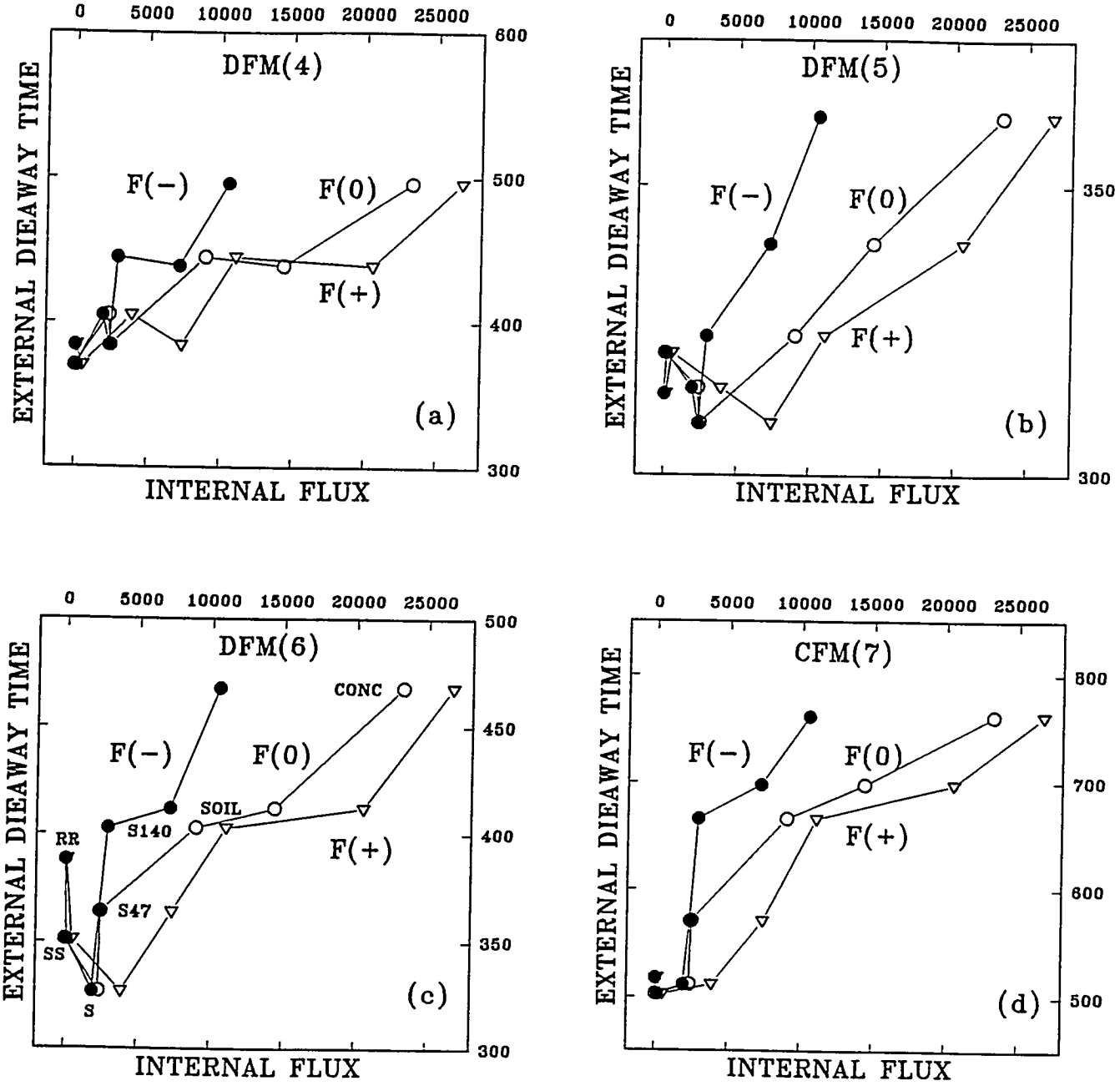

INTERNAL FLUX VERSUS EXTERNAL DIEAWAY TIMES

FIGURE 7

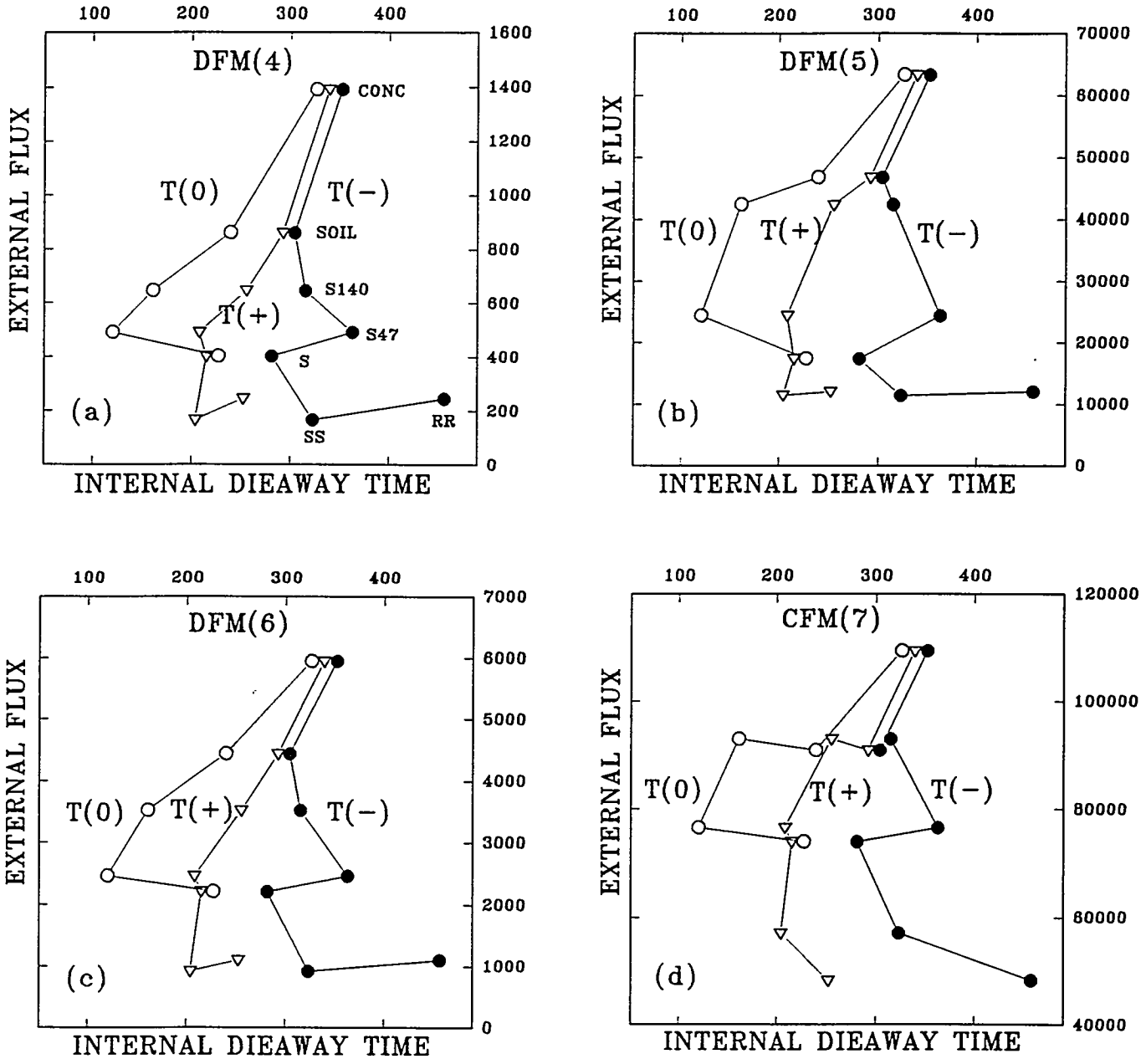

INTERNAL DIEAWAY TIME VERSUS EXTERNAL FLUX

FIGURE 8

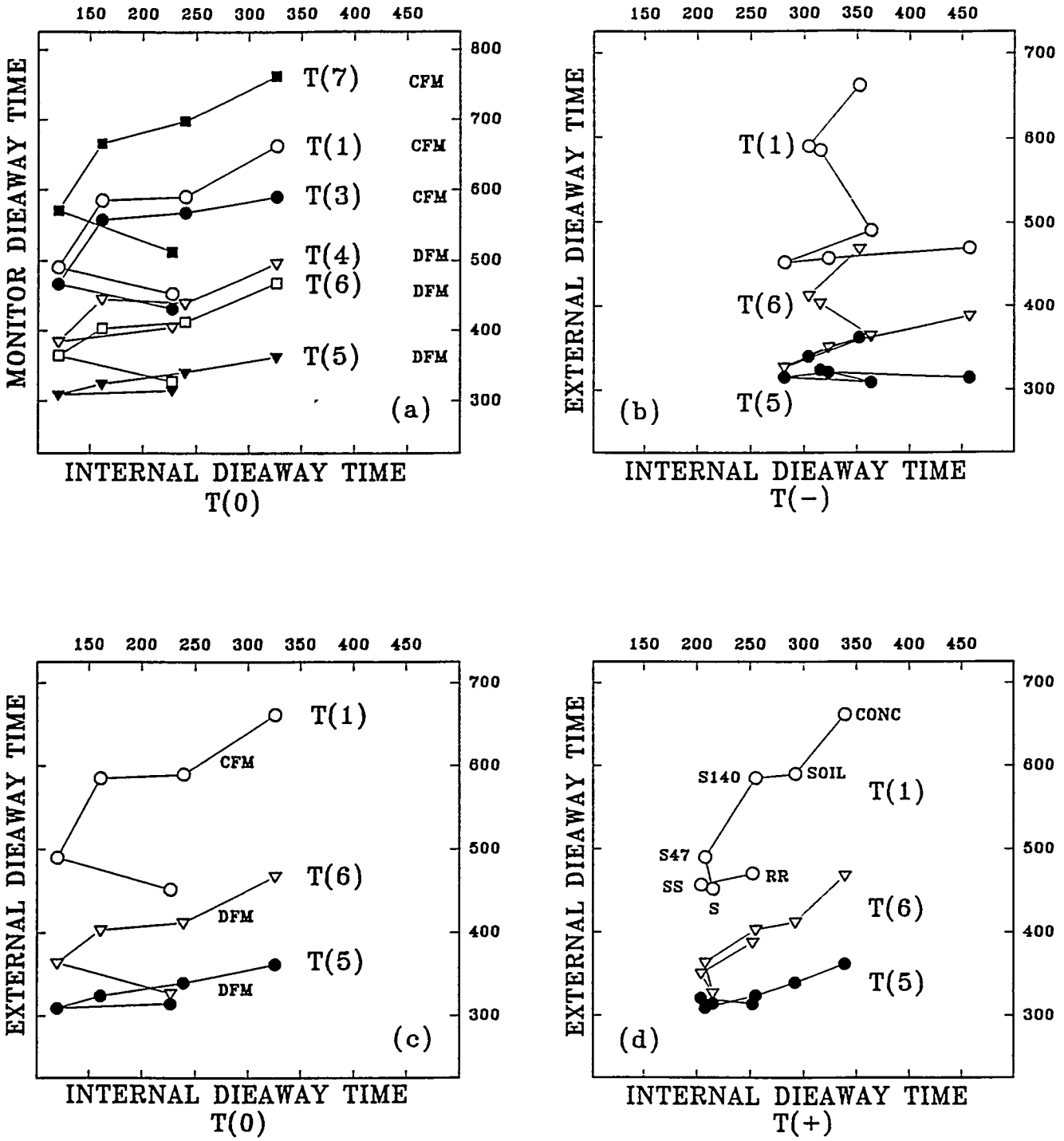

INTERNAL DIEAWAY TIMES VERSUS EXTERNAL DIEAWAY TIMES

FIGURE 9

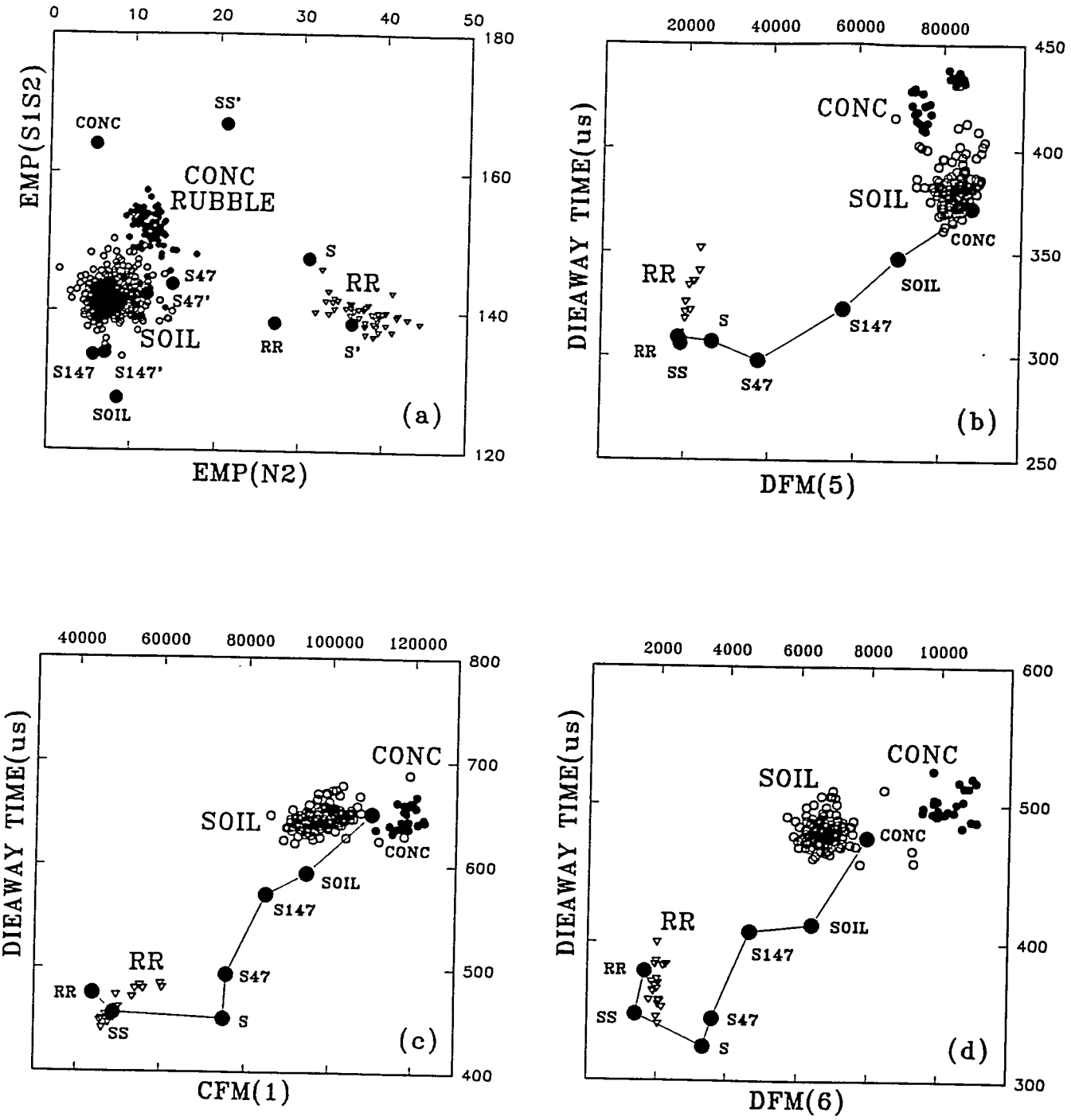

Efficiency and Flux Matrix Determination

Figure 10